Supporting Information

Masuda-Nakagawa et al. 10.1073/pnas.0900178106

SI Text

Immunocytochemistry. The CNS of wandering third-instar larvae was dissected in phosphate buffer (PBS), fixed, and labeled as described (1). Primary antibodies were: mouse 4F3 anti-Dlg (2) (1:200), rabbit anti-GFP (1:1,000; Molecular Probes), and mouse anti-Myc 9E10 (3) (1:20). Secondary antibodies were anti-mouse Alexa 647 (1:200; for anti-Dlg) and anti-rabbit Alexa 488 (1:200; for anti-GFP) or in case of *Or83b-Myc*, anti-mouse 568 (1:200; for both anti-Myc and anti-Dlg) and anti-rabbit Alexa 488 (1:200 for anti-GFP). Antibody incubations were performed on a rotating shaker for 2 nights at 4 °C. Brains were kept in 50% glycerol overnight and mounted in 50% glycerol in PBS under a coverslip supported by strips of electric insulation tape 0.2 mm thick × 19 mm wide × 10 mm long), to protect the anatomy of the CNS.

Specimen Orientation and Confocal Immunomicroscopy. Orientation of the larval AL was defined relative to the body axis rather than the neuraxis. Accordingly, the AL is situated at the anterior edge of the brain, similar to the adult fly (Fig. S2). Images of the AL were taken in the frontal plane of the brain, from anterior to posterior. Standardized orientation was obtained by adjusting specimens under the microscope to include in the same optical section the most anterior levels of the AL and the prominent anterior protrusion of the MBs, the lateral appendix, close to the intersection between the MB lobes (Fig. S2). Optical sections usually contained the same levels of the left and right ALs and other conspicuous brain structures (such as the MB lobes). Occasional tilt, i.e., a difference of 2–4 optical sections between corresponding left and right structures, or a rotation of the brain around the mediolateral (ML) axis, which caused the AL to be included in more anterior sections than the MB lateral appendix, were taken into account for glomerular identification. Neither nc82 anti-BRP (4), a standard marker for adult AL glomeruli (5), nor labeling AL glia using *Nrv2-GAL4* (6) or anti-Draper (7) improved resolution of glomerular boundaries beyond that seen using anti-Dlg.

Stacks of confocal pictures were taken either by using a Bio-Rad MRC 1024 mounted on a Nikon Eclipse E800 with a Plan Apo 60x/1.40 Oil Dic H /0.17 WD 0.21 objective and voxel size 0.08 × 0.08 × 1.0 μm (x, y, z), or a Zeiss LSM510 with a C-Apochromat 40x/NA1.2 W objective and voxel size 0.23 × 0.23 × 0.69 μm (x, y, z). Images were cropped and processed by using ImageJ (http://rsb.info.nih.gov/ij) and Photoshop (Adobe Systems) software. Minimum and maximum levels and gamma settings were adjusted across the entire image to improve contrast between glomeruli and background, and in most images a median filter (radius 1 pixel) was used to reduce background noise.

3D glomerular reconstruction of the larval AL was based on the patterns of OSN terminals visualized by 22 *OrX-GAL4* lines in at least 12 ALs, from 6 or more brains per line. Center positions were estimated by placing the center of each glomerulus from each individual in a grid of 17 levels each in the dorsoventral (DV) and ML levels and 7 levels in the anteroposterior (AP) axis. The lengths of the DV (31.6 ± 3.6 μm) and ML (32.6 ± 3.5 μm) axes of the larval AL exceed that of the AP (23.5 ± 1.3 μm) axis (mean ± SD; n = 241). For a 3D, outlines of individual glomeruli were drawn as a multilayered tif file in 27 1-μm optical sections in the AP axis. Glomerular shapes and sizes were drawn by averaging the most representative OSN terminal patterns. A 3D reconstruction of the averaged AL map was generated by using Amira (Visage Imaging GmbH, Düsseldorf, Germany), with each section replicated a total of 5 times along the z axis before interpolation. ALs in the left hemisphere were mirrored to appear as if they were in the right hemisphere. 3D reconstruction of the calyx map was performed by using 0.6-μm sections of a single calyx labeled with anti-Dlg and *UAS-nsyb::GFP* under control of *GH146-GAL4*.

Imaging Neuronal Activity in Calyx. The parental *GC56*;*OrX-GAL4*;*or83b*^{1} stocks used for the imaging crosses were verified by visualizing GFP expression in the AL (Fig. S8) and showed similar morphology of labeling in AL glomeruli as the same *OrX-GAL4* insertions in an *or83b*$^{+}$ background (Figs. S1 and S5).

GCaMP fluorescence was visualized by using a CSU22 spinning disc confocal (Yokogawa Electric Corporation) mounted on an Axioplan 2 microscope (Zeiss), and captured with a CoolSNAP HQ CCD camera (Photometrics). Exposure times were 200 ms and frame rates were 1 per 270 ms. Acquisition and camera control was carried out by using Slidebook (version 4.1.0.6; Intelligent Imaging Innovations). Before acquisition, larvae were exposed to a stream of air at 60 mL/min, delivered through Tygon tubing [internal diameter (ID) 1 mm; Saint Gobain Corporation). Air was pumped from an OP-N026 aquarium pump (Iwaki) through a series of 3 1-L bottles containing cotton wool, charcoal, and water connected by Tygon tubing (ID 7 mm), to an RK1200 flowmeter (Kofloc). Air from the flowmeter passed through Teflon tubing (ID 2 mm; DuPont) to an MTV-3-NM6 3-way valve (Takasago), a bubbler containing 2 mL of mineral oil, a Warner MP-2 manifold, and a needle (ID 0.8 mm) directed at the larva. Initiation of imaging triggered a TTL pulse from the camera to a Master-8-cp stimulator (AMPI), which after a delay of 2 s, switched the 3-way valve to divert the airflow from the bubbler with mineral oil, to an alternative bubbler with odorant diluted to 10% in paraffin oil, from where it passed to the manifold and the larva. Odorant was delivered for 2 s, after which the 3-way valve was switched back to the nonodorant channel. Ethyl acetate (ACS reagent ≥99.5%), acetophenone (ReagentPlus grade, 99%) and paraffin oil (IR spectroscopy grade) were obtained from Sigma–Aldrich.

To display ΔF and calculate $\Delta F/F$, Slidebook files were converted to 8-bit Quicktime movies (Codec H.264, high quality). Images were corrected for fluorescence decay by using the ImageJ plug-in Stacks T-functions Bleach Correction (www.macbiophotonics.ca/imagej/t.htm). Where necessary, the first or last few frames were removed before bleach correction to improve the fit to exponential decay. A resting fluorescence image was generated by averaging 3–6 unstimulated frames, and this was subtracted from each frame of the bleach-corrected movie to generate a movie of ΔF. Pixel noise was reduced by filtering images with a Gaussian Blur (radius 1 pixel). The movie was displayed by using the Rainbow2 lookup table (LUT), and the minimum and maximum levels were adjusted to remove most low-level random fluorescence fluctuations between frames and to use most of the LUT range for display. To plot a time course of $\Delta F/F$, a region of interest (ROI) was defined along the edge of an active glomerulus in an unprocessed 8-bit movie, and a time course of average fluorescence was calculated. $\Delta F/F$ was calculated relative to the starting fluorescence, normalized to the fluorescence decay in an ROI in a large unresponsive region of the preparation. A variable lag phase was observed between the programmed odor pulse and the calyx response, presumably caused by variability in the orientation of the dissected larval preparation relative to the odor stream. To allow for this, $\Delta F/F$

traces from different individuals were aligned around the time point at which the steepest increase in ΔF/F was observed; and the average period of the odor pulse was shown on graphs that plotted the average time course of ΔF/F.

In the absence of any functional OSN input (larvae carrying *GH146-GAL4* and *UAS-GCaMP1.3* in an *or83b*^{1} mutant background), no activity was ever observed in the calyx in response to either ethyl acetate (16 calyces observed in 11 different larvae) or acetophenone (19 calyces from 10 larvae), confirming that calyx activity depended on OSN input. In a number of these preparations, a *GH146*-expressing projection beneath the calyx showed weak activity (ΔF/F ≈4%) in response to both ethyl acetate and acetophenone. Because *GH146*-GAL4 is expressed also outside PNs and the *or83b*^{1} mutation abolishes all detectable olfactory input from OSNs (8), this effect was likely caused by nonolfactory effect of odor delivery. However, we could not trace the origin of the activated projection.

1. Masuda-Nakagawa LM, Tanaka NK, O'Kane CJ (2005) Stereotypic and random patterns of connectivity in the larval mushroom body calyx of *Drosophila*. *Proc Natl Acad Sci USA* 102:19027–19032.
2. Parnas D, Haghighi AP, Fetter RD, Kim SW, Goodman CS (2001) Regulation of postsynaptic structure and protein localization by the Rho-type guanine nucleotide exchange factor dPix. *Neuron* 32:415–424.
3. Evan GI, Lewis GK, Ramsay G, Bishop JM (1985) Isolation of monoclonal antibodies specific for human *c-myc* protooncogene product. *Mol Cell Biol* 5:3610–3616.
4. Wagh DA, et al. (2006) Bruchpilot, a protein with homology to ELKS/CAST, is required for structural integrity and function of synaptic active zones in *Drosophila*. *Neuron* 49:833–844.
5. Laissue PP, et al. (1999) Three-dimensional reconstruction of the antennal lobe in *Drosophila melanogaster*. *J Comp Neurol* 405:543–552.
6. Sun B, Xu P, Salvaterra PM (1999) Dynamic visualization of nervous system in live *Drosophila*. *Proc Natl Acad Sci USA* 96:10438–10443.
7. Freeman MR, Delrow J, Kim J, Johnson E, Doe CQ (2003) Unwrapping glial biology: Gcm target genes regulating glial development, diversification, and function. *Neuron* 38:567–580.
8. Fishilevich E, et al. (2005) Chemotaxis behavior mediated by single larval olfactory neurons in *Drosophila*. *Curr Biol* 15:2086–2096.

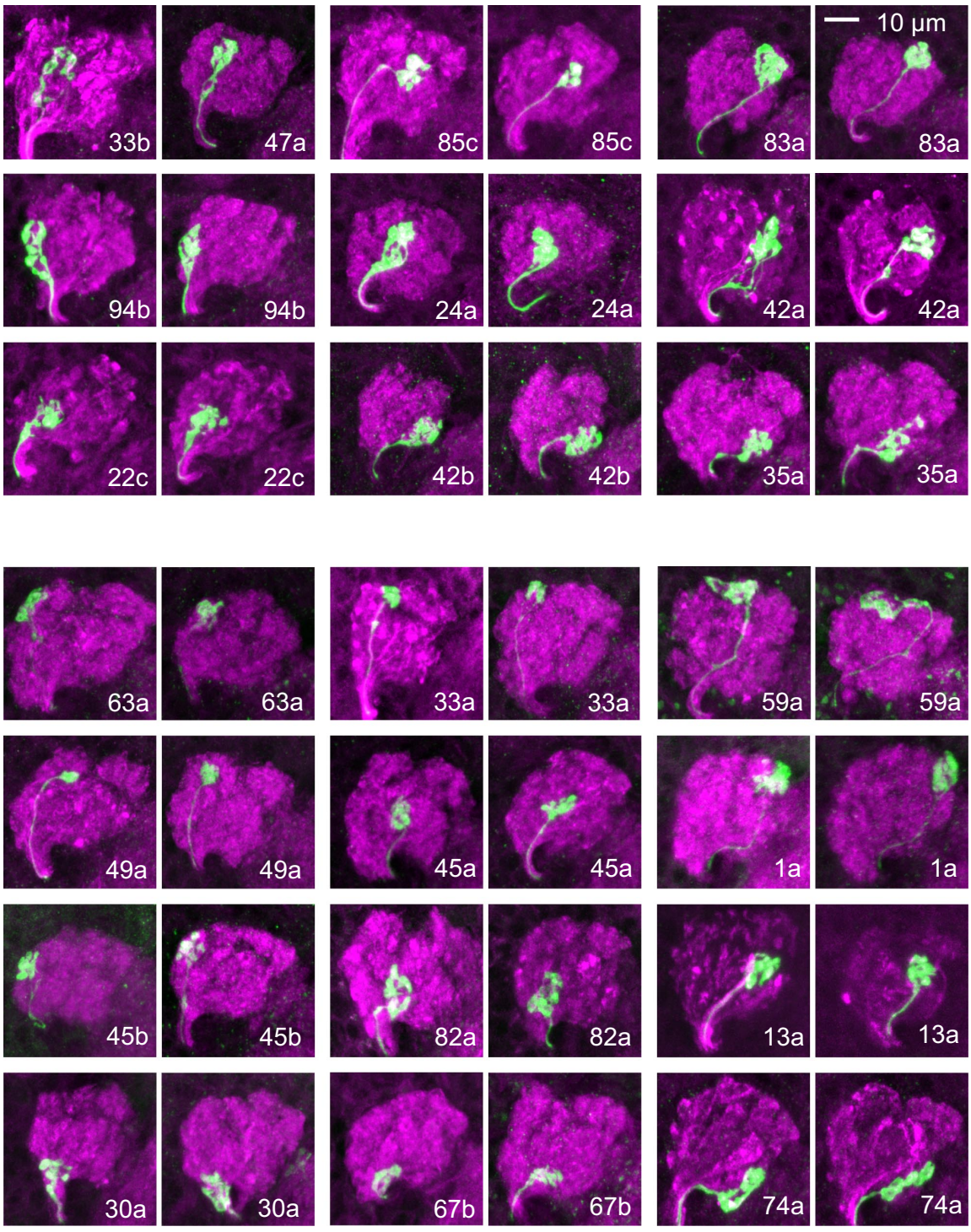

Fig. S1. OSN terminals in the larval AL. Larvae carrying *OrX-GAL4*, *UAS-GFP*, and *Or83b-Myc* were labeled by using anti-GFP (green) to visualize OSN projections and anti-Dlg and anti-Myc (both magenta) to visualize the organization of the AL. Shown are projections of confocal sections; in this and all subsequent figures, AL sections are viewed from anterior (for orientation see Fig. S2), with dorsal to the top and lateral to the left. The panels on top show glomeruli in the anterior part of the AL, the lower panels show glomeruli in the middle and posterior parts. For each *OrX-GAL4* line, 2 examples are shown illustrating the type of variability observed; for *Or33b* and *Or47a*, which are coexpressed in the same OSN, only 1 example each is shown. The arrangement of individual panels in the top and bottom groups reflects the location of the glomeruli inside the AL. The sensory terminals consist of branches and varicosities of variable numbers, size, and shape.

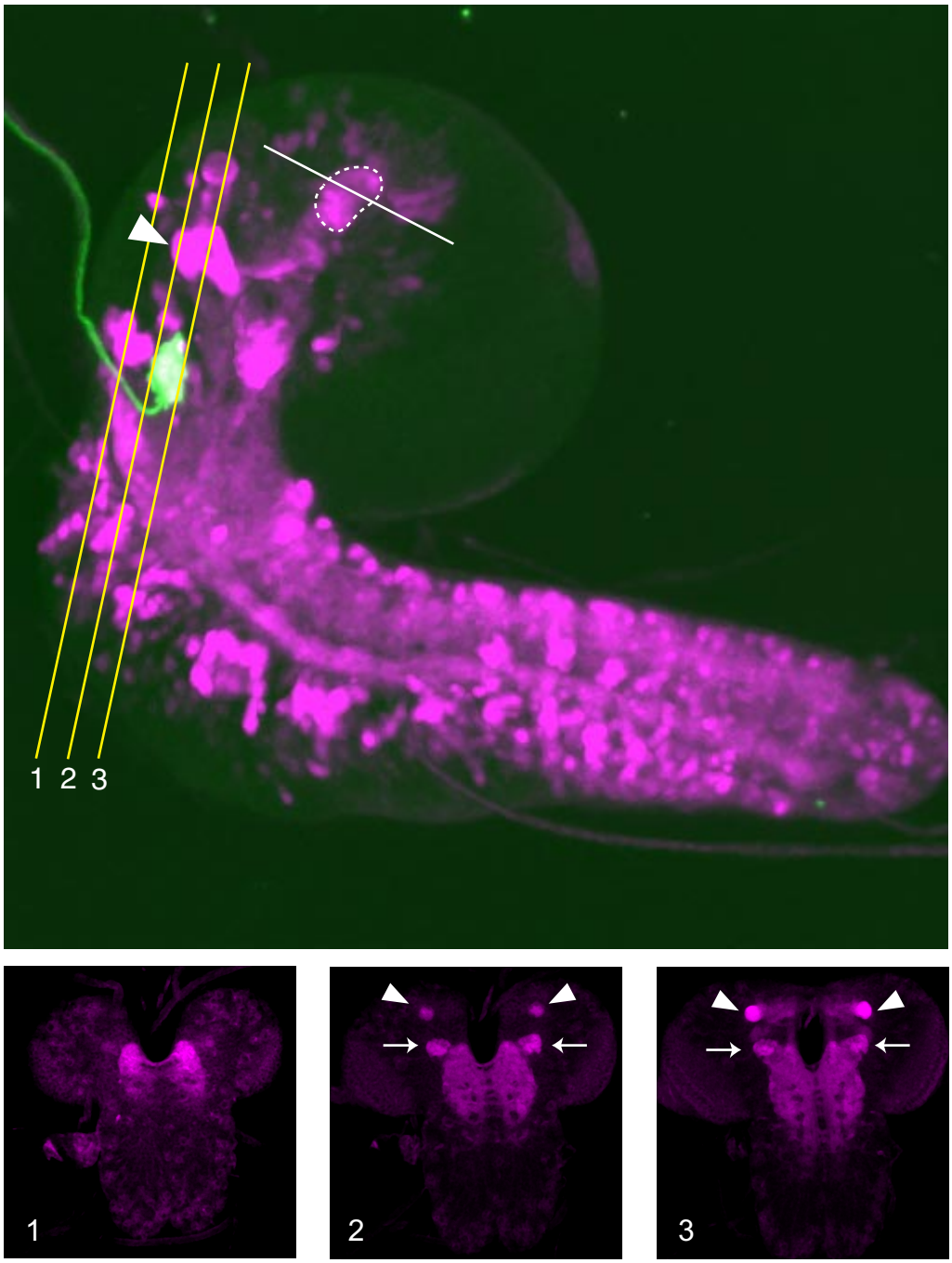

Fig. S2. Lateral view of the larval CNS showing the projections of OSNs in the AL (*Or83b-GAL4xUAS-GFP*; green) in a background stained by *Gad1-RFP* (magenta) (www.ncbi.nlm.nih.gov/projects/geo/query/acc.cgi?acc = GSE1048). The yellow and white lines refer to the confocal planes used, respectively, for mapping OSN terminals in the AL, and PN projections in the MB calyx (stippled contour). The panels below correspond to the 3 yellow lines. In the standard orientation used for mapping OSN terminals, confocal sections (2, 3) comprised both the AL (arrows) and the lateral appendix of the MBs (arrowheads).

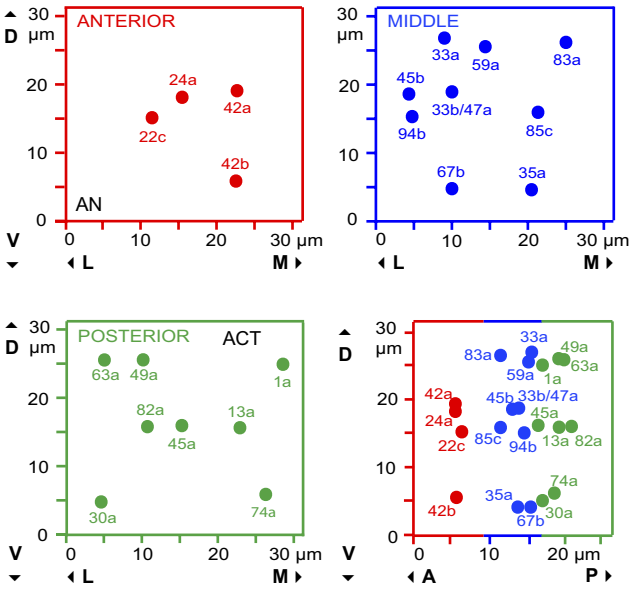

Fig. S3. Average center positions of glomeruli in the larval antennal lobe represented as a 3D grid. Positions were calculated from the average locations of OSN terminals in 22 *OrX-GAL4* lines, each assessed in a minimum of 12 ALs. The first 3 panels are frontal views of different levels along the AP axis; the last panel is a medial view. The centers of glomeruli at the anterior, middle, and posterior levels along the AP axis are represented by red, blue, and green, respectively. For the means and standard deviations of the center positions, see Table S1. AN, antennal nerve entry; ACT, antennocerebral tract exit.

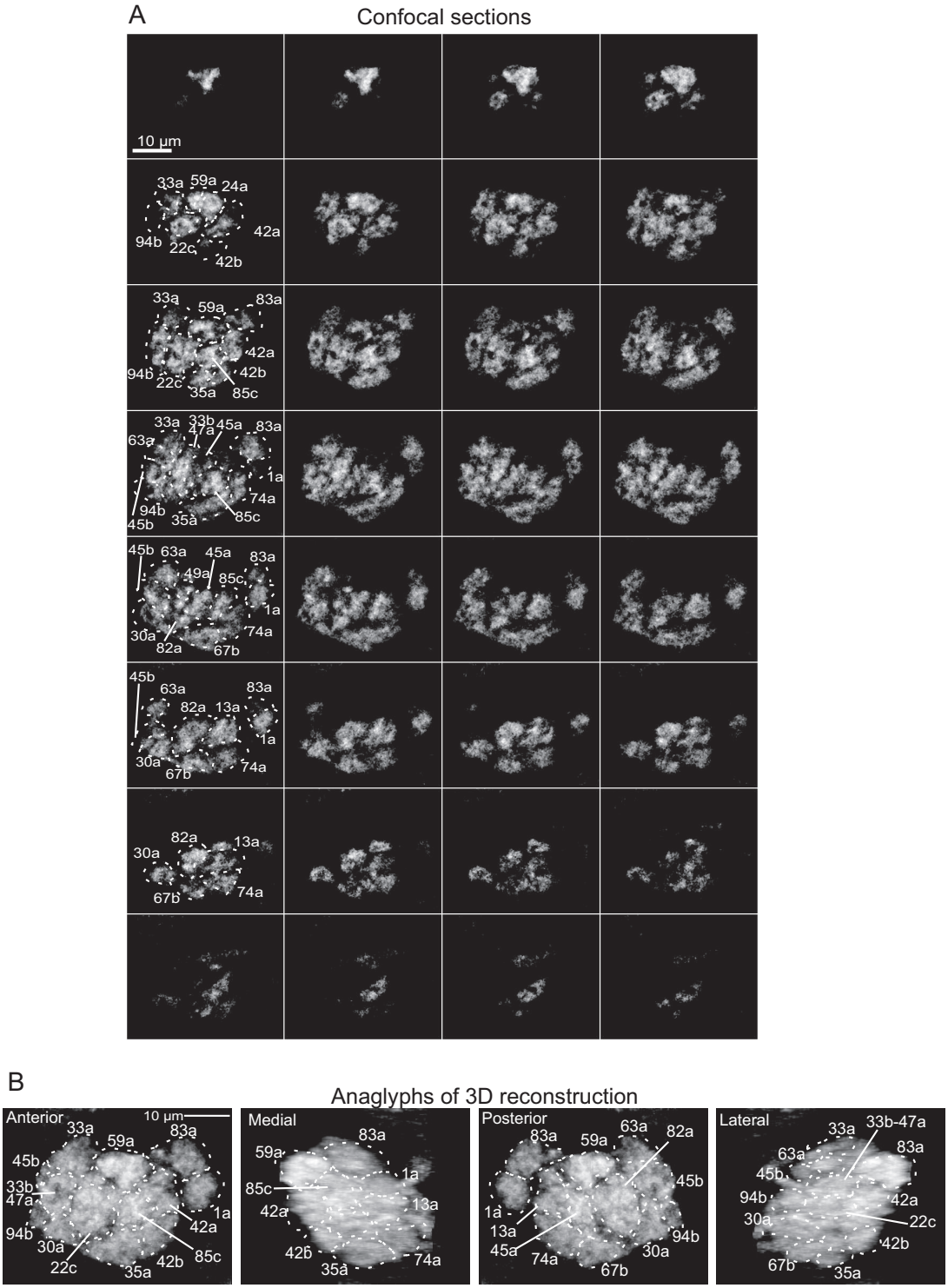

Fig. S4. (*A*) A complete series of frontal sections at 1-μm steps through the same AL as shown in Fig. 1*D*. Labeling is anti-Dlg. Glomeruli are labeled and outlined with broken lines. (*B*) 3D reconstruction of the larval AL shown in Fig. 1*D*, viewed from different angles, and shown as anaglyphs that can be visualized with glasses with red (left pane) and blue, green or cyan (right pane) filters. Lateral and medial views are oriented so that the anterior surface of the AL is tilted slightly toward the reader. Glomeruli closest to the reader are outlined with broken lines. A full rotation of the reconstruction is shown in Movie S1.

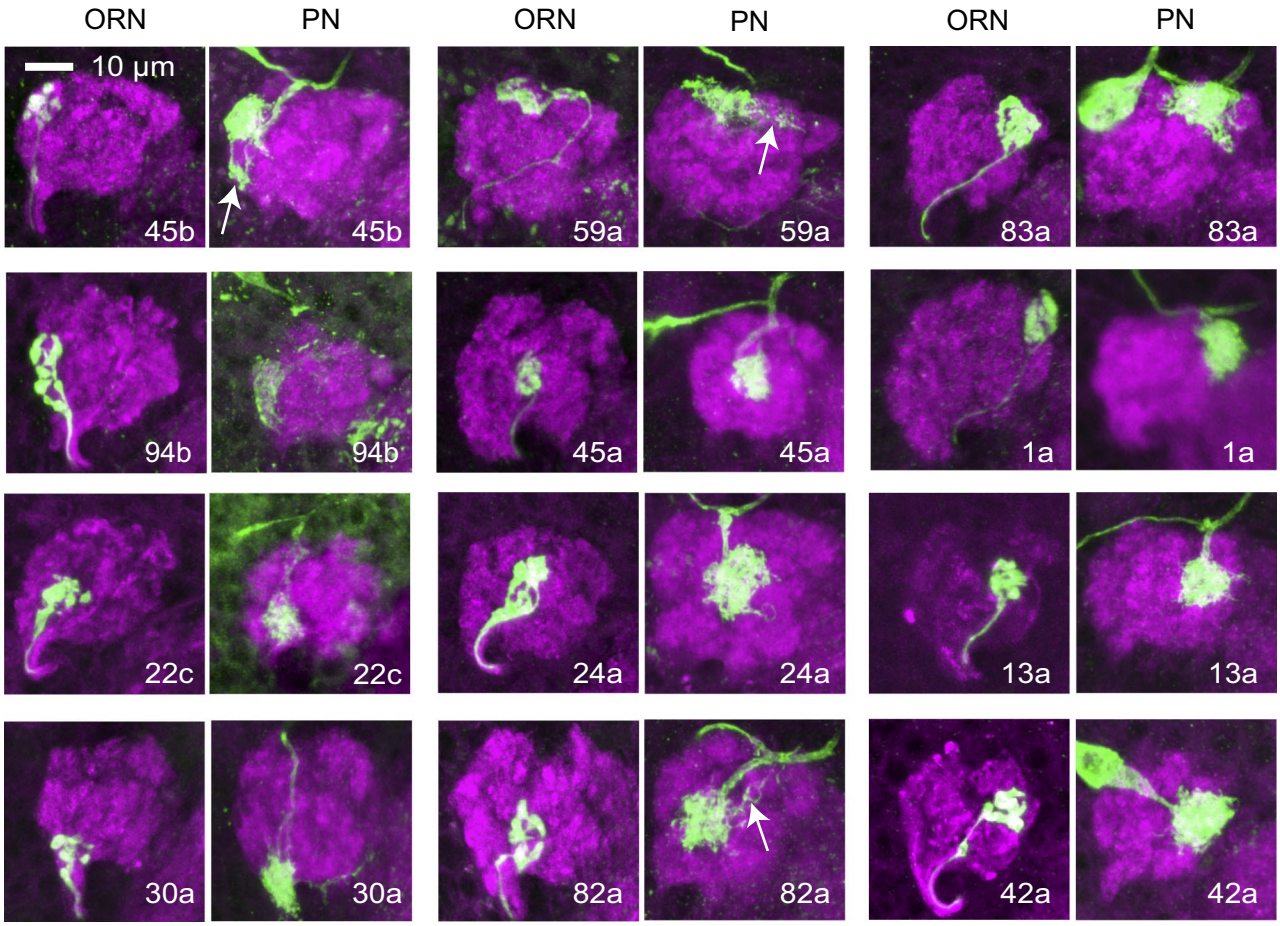

Fig. S5. Matching positions of OSN terminals and PN dendritic arbors in 12 selected glomeruli in the larval AL. The OSN terminals shown are the same as those in Fig. S1. Single PN clones were labeled by using *mCD8*::*GFP*, expressed using FLP-out recombination in *GH146-GAL4* larvae, and stained with anti-Dlg (magenta). In general, PNs cover larger areas than OSN terminals and sometimes spill over into neighboring glomeruli (examples shown by arrows). The arrangement of panels is according to the location of the glomeruli in the AL.

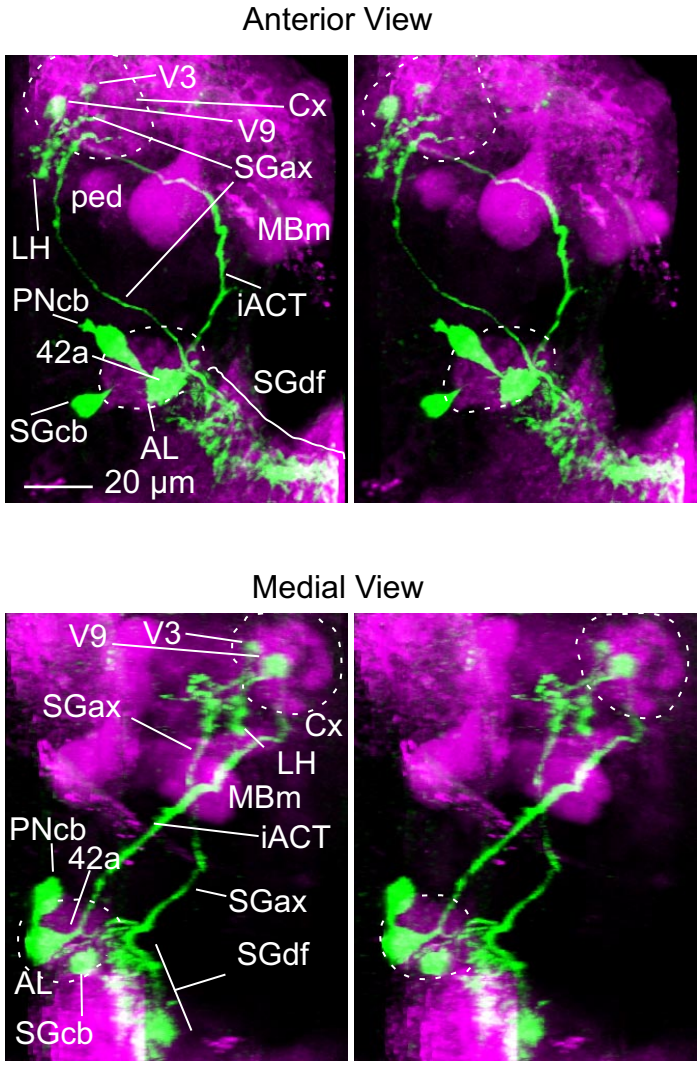

Fig. S6. Innervation of calyx glomerulus V3 by a neuron originating in the suboesophageal ganglion. The panels are stereo pair images of the preparation used in the left pair of panels showing AL glomerulus 42a and calyx glomerulus V9 in Fig. 2, viewed from approximately anterior (top pair) and medial (bottom pair) directions. Two neurons (green) innervate the calyx: a PN projects from its cell body (PNcb) to AL glomerulus 42a and via the inner antennocerebral tract (iACT) to calyx glomerulus V9 and the lateral horn (LH); a non-PN neuron projects from its cell body (SGcb) to its dendritic field (SGdf) in the suboesophageal ganglion and via its axon (SGax) to calyx glomerulus V3. The calyx (Cx), AL (broken lines) and other neuropil are visualized using anti-Dlg (magenta). MBm, mushroom body medial lobe; ped, pedunculus. Nonspecific staining of the green channel on some parts of the brain surface has been removed before 3D reconstruction, to avoid obscuring the internal projections of neurons expressing *mCD8*::*GFP*. A complete rotation of this reconstruction around the DV axis is shown in Movie S4.

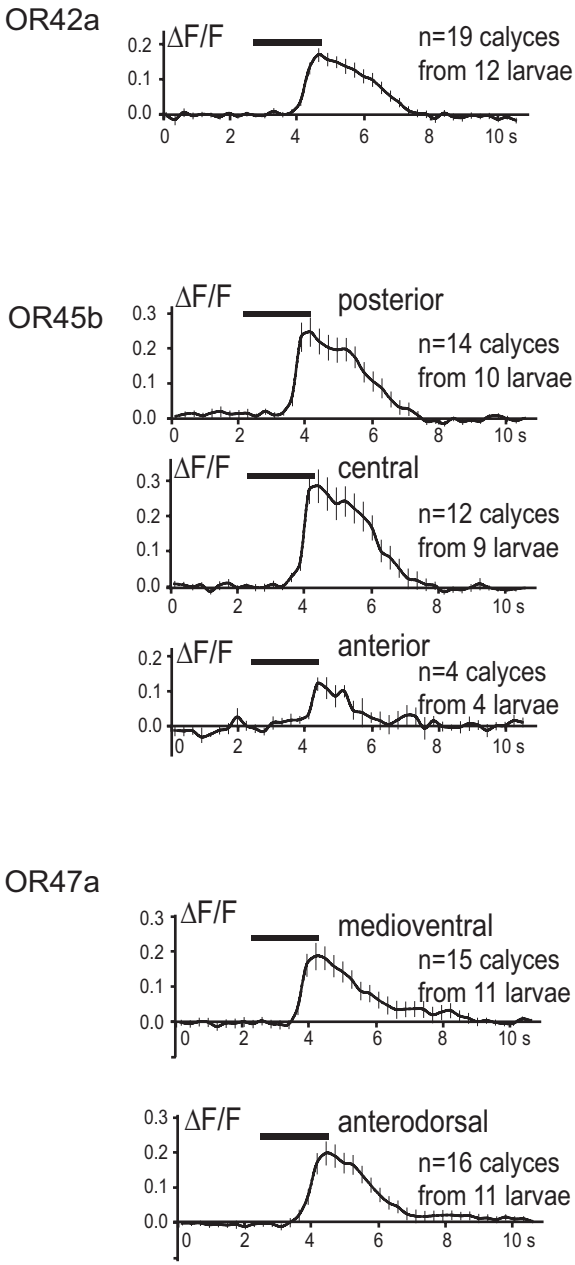

Fig. S7. Time course and magnitude of ΔF/F in calyx glomeruli activated by single OSN inputs (mean ± SEM). Examples of glomeruli used are seen in Fig. 4. Horizontal bars show the approximate duration of odor delivery.

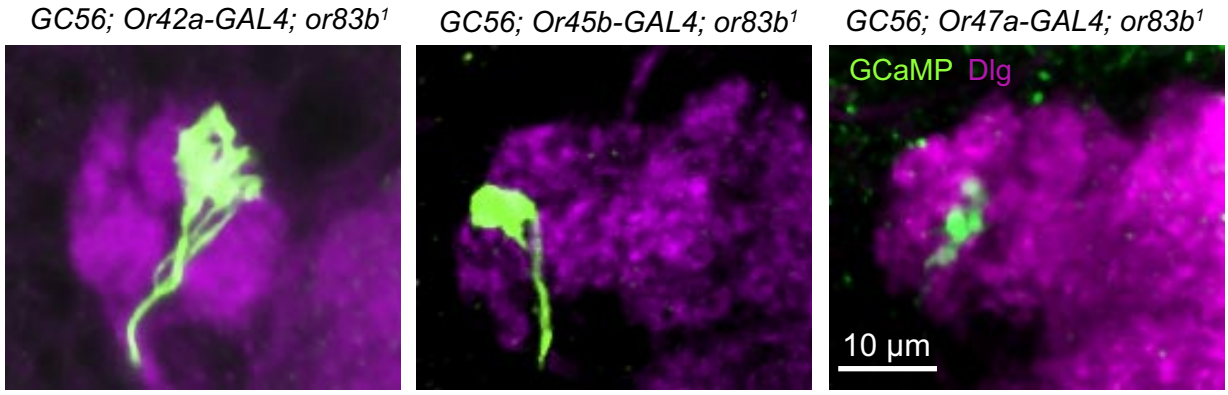

Fig. S8. Expression of GFP in the expected AL glomeruli in the *UAS-GCaMP1.3(GC56);OrX-GAL4;or83b*^{1} parental stocks used for the imaging crosses.

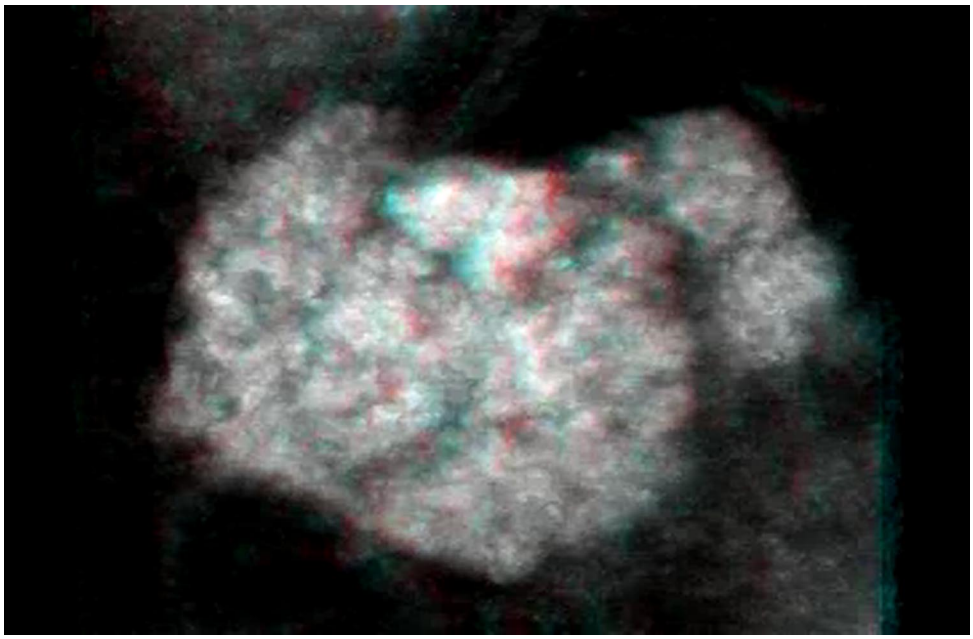

Movie S1. A complete rotation around the DV axis of the 3D reconstruction of a larval AL shown in Fig. S4*B*.

Movie S1 (MOV)

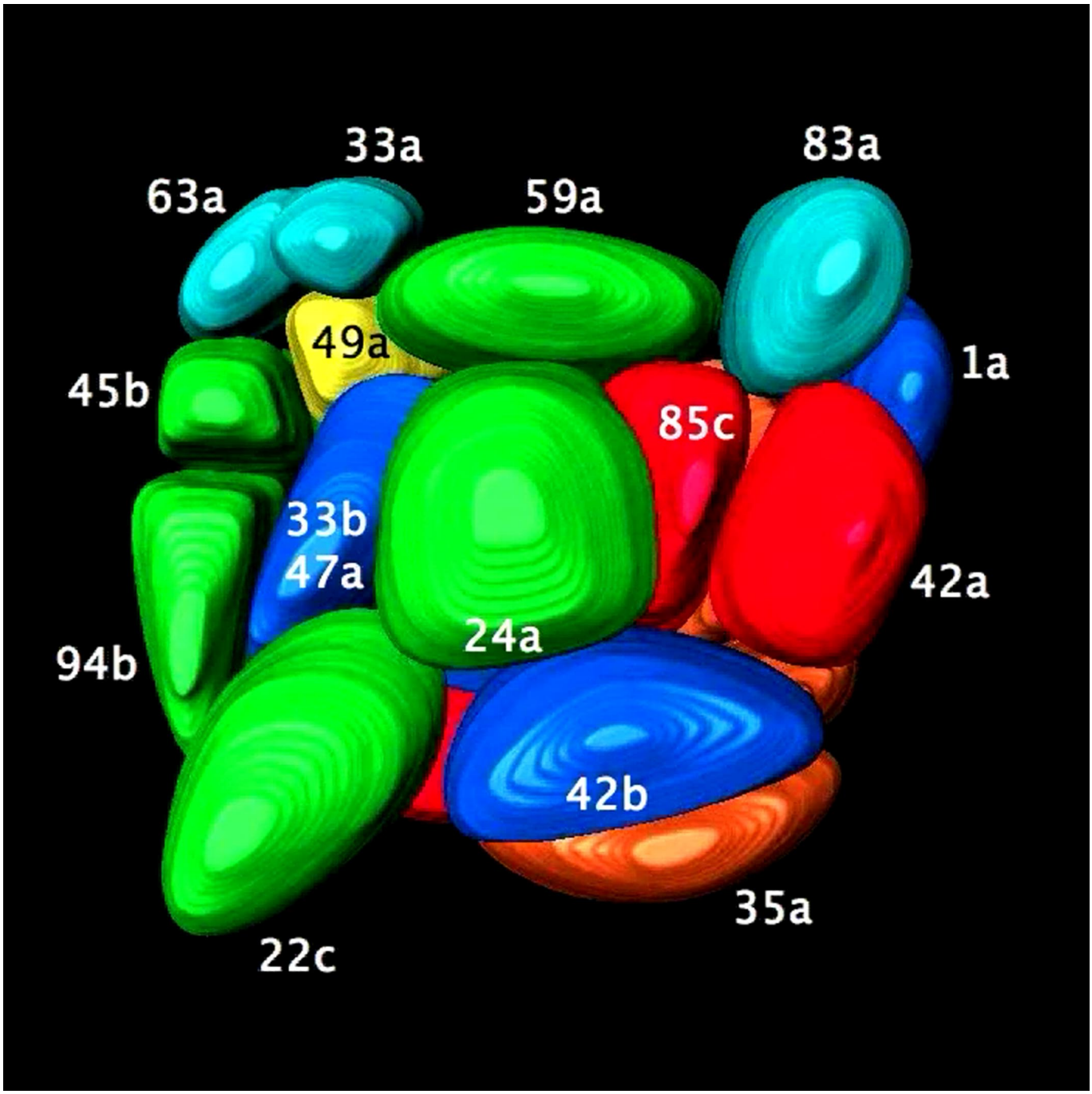

Movie S2. A complete rotation around the DV axis of the 3D AL model shown in Fig. 1*E*.

Movie S2 (MOV)

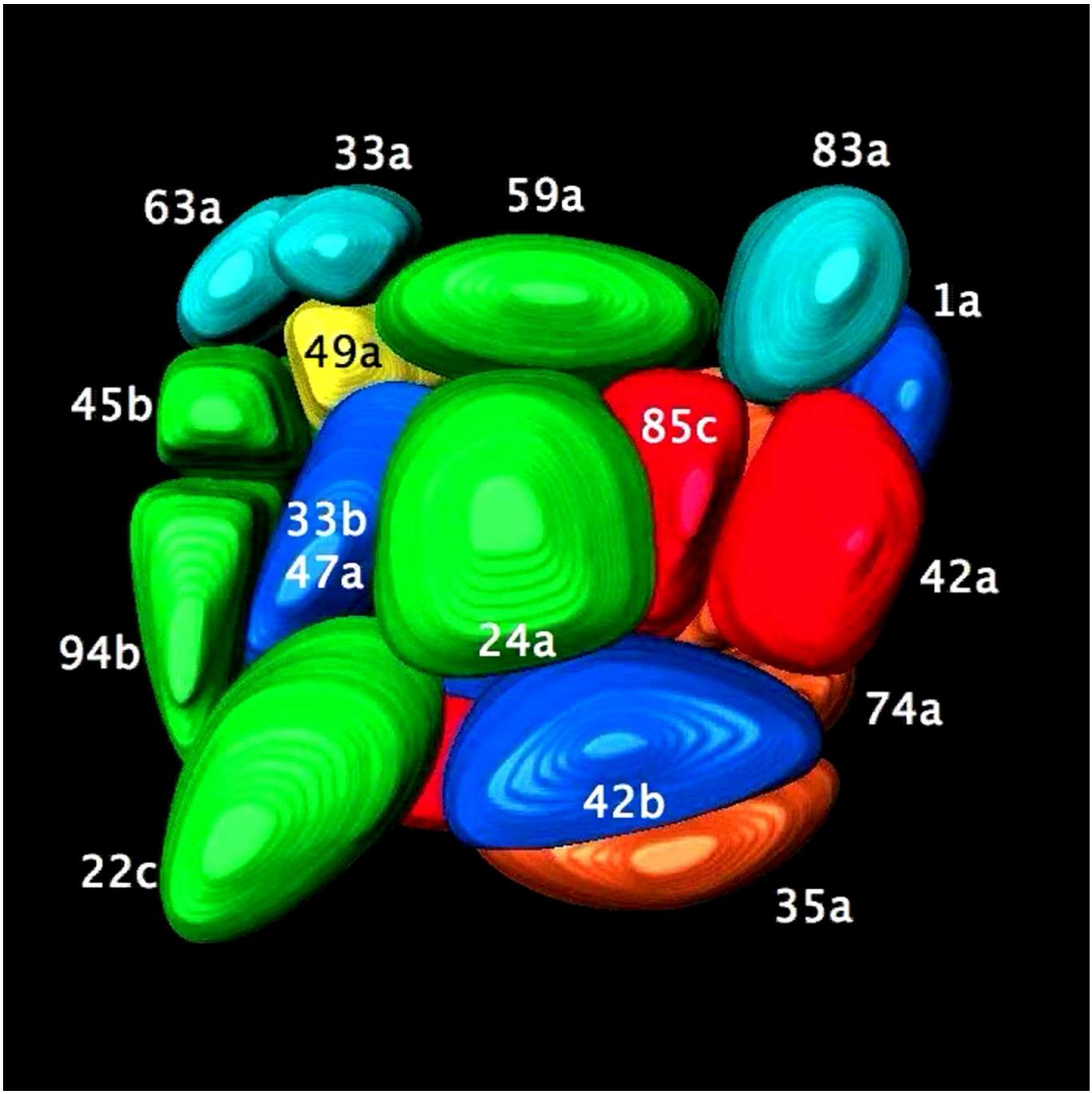

Movie S3. A complete rotation around the ML axis of the 3D AL model shown in Fig. 1*E*.

Movie S3 (MOV)

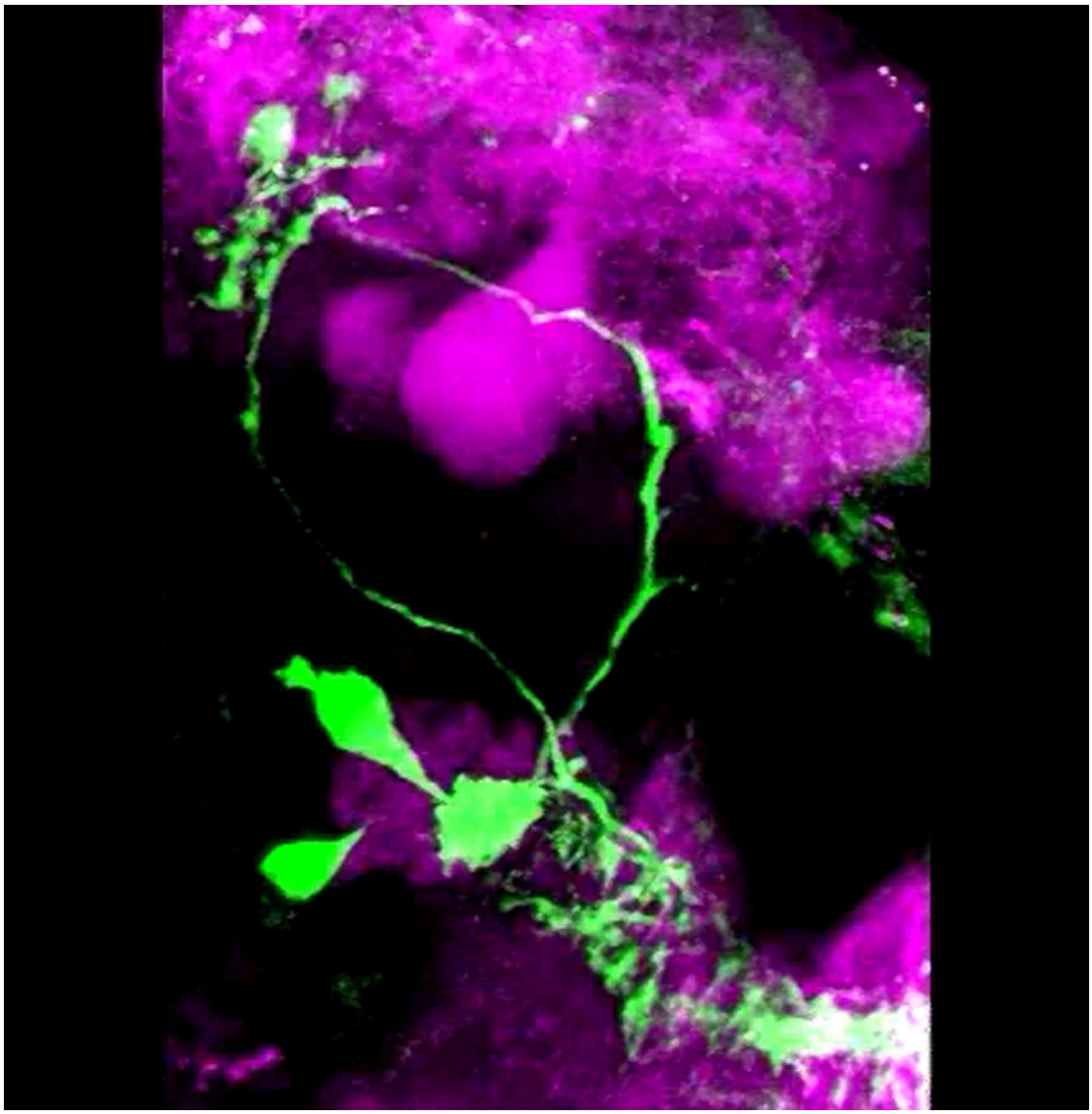

Movie S4. A complete rotation around the DV axis of the brain hemisphere shown in Fig. S6.

Movie S4 (MOV)

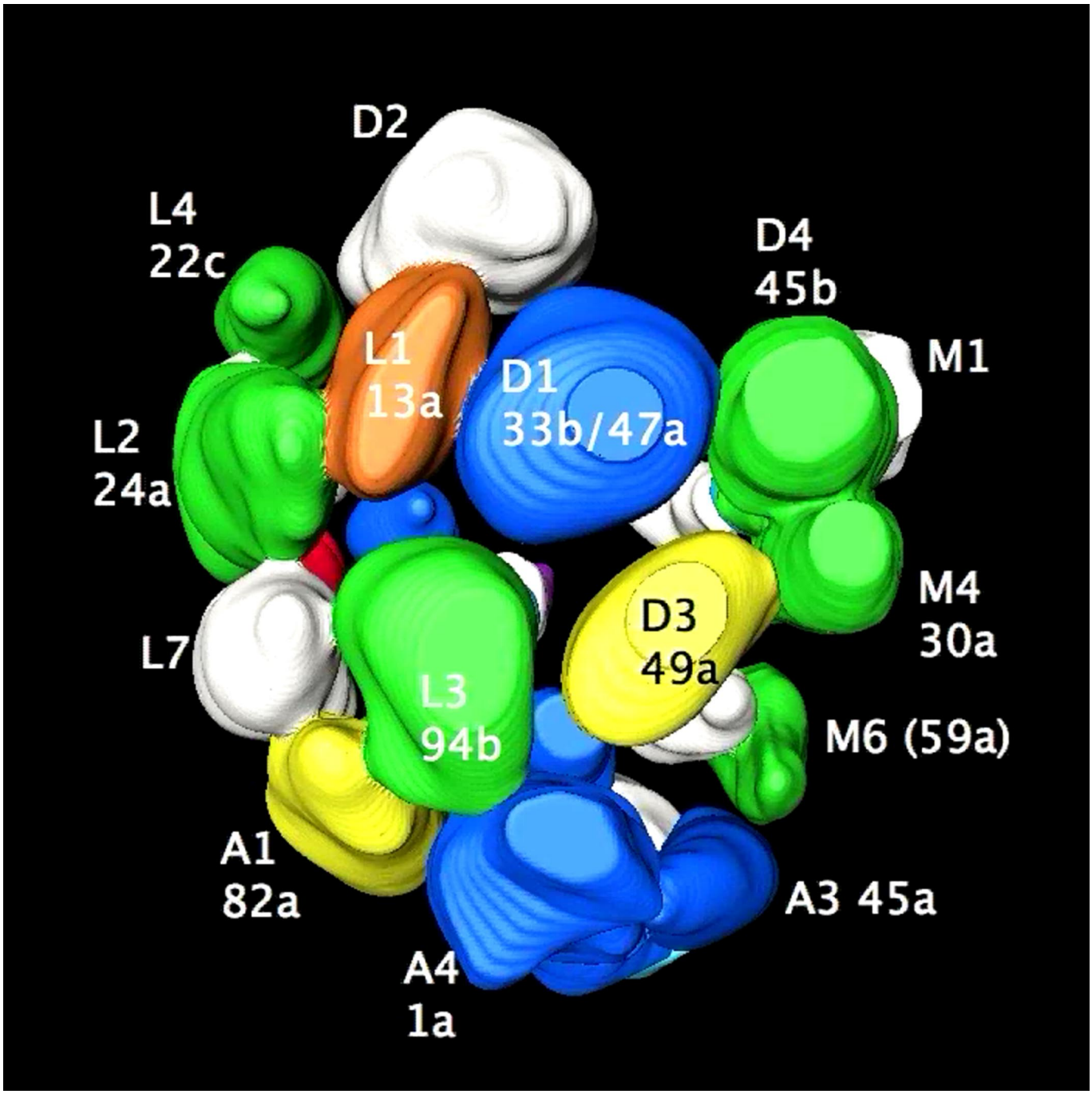

Movie S5. A complete rotation around the AP axis of the calyx model shown in Fig. 3.

Movie S5 (MOV)

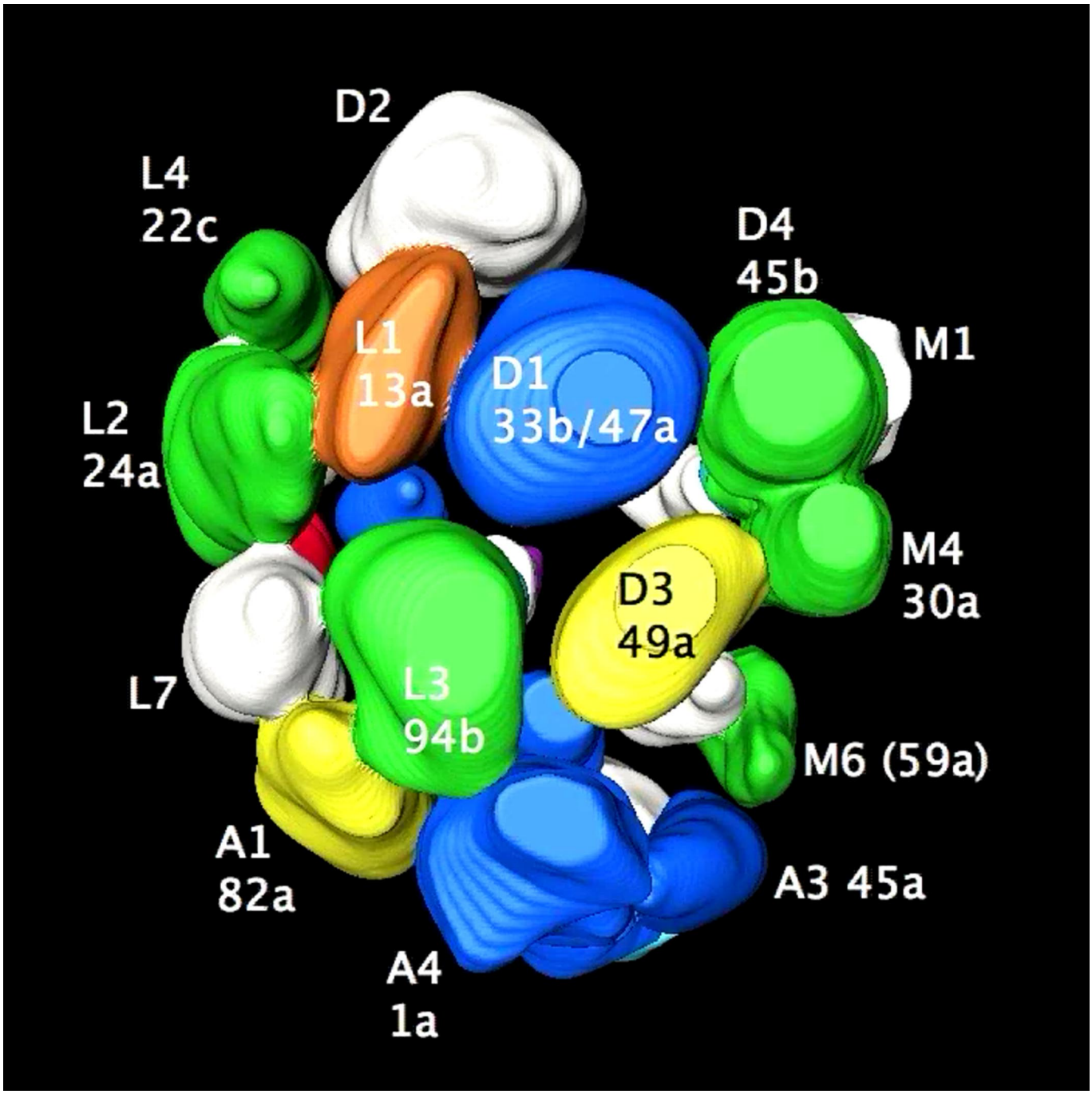

Movie S6. A complete rotation around the ML axis of the calyx model shown in Fig. 3.

Movie S6 (MOV)

Table S1. Positions of individual larval AL glomeruli

Glomerulus	Lateral-medial	Ventral-dorsal	Anterior-posterior	*n*
1a	27.5 ± 1.7	24.7 ± 1.6	17.0 ± 1.5	12
13a	22.0 ± 0.0	15.8 ± 0.6	18.8 ± 1.9	12
22c	11.5 ± 2.6	14.9 ± 1.3	6.7 ± 1.8	13
24a	16.0 ± 2.6	18.5 ± 2.7	6.3 ± 0.9	12
30a	4.0 ± 0.0	4.7 ± 1.3	16.5 ± 2.3	14
33a	9.0 ± 1.8	26.6 ± 2.5	15.8 ± 3.4	16
33b	9.8 ± 0.6	19.2 ± 2.0	13.8 ± 2.0	12
35a	21.2 ± 1.4	4.2 ± 0.6	12.8 ± 2.3	18
42a	21.8 ± 1.3	18.7 ± 3.1	6.0 ± 0.0	12
42b	21.5 ± 2.3	6.0 ± 0.0	6.0 ± 0.0	12
45a	14.7 ± 1.0	16.0 ± 0.0	17.3 ± 1.4	12
45b	4.3 ± 1.1	18.3 ± 2.8	14.8 ± 2.3	13
47a	10.0 ± 0.0	18.0 ± 2.7	13.0 ± 2.7	12
49a	9.7 ± 0.8	26.7 ± 2.5	18.8 ± 3.6	12
59a	12.9 ± 3.1	25.2 ± 1.0	15.2 ± 1.4	15
63a	5.5 ± 2.4	26.1 ± 4.0	19.0 ± 2.4	15
67b	9.7 ± 0.8	4.0 ± 0.0	15.2 ± 2.3	13
74a	26.3 ± 2.1	6.0 ± 2.0	18.0 ± 1.2	13
82a	10.7 ± 1.6	15.7 ± 0.8	21.0 ± 0.0	12
83a	25.1 ± 3.2	27.1 ± 2.2	12.2 ± 3.0	14
85c	21.9 ± 0.5	16.4 ± 1.5	11.7 ± 2.0	18
94b	4.5 ± 0.9	14.5 ± 2.3	13.0 ± 2.7	12

Data show the mean and standard deviation of the position of the center of gravity of each AL glomerulus, expressed as distance in μm from the extreme lateral, ventral, and anterior planes of the whole AL.

Table S2. Antennal lobe and calyx glomeruli innervated by individual projection neurons

AL*	Calyx*	Main OSN sensitivity†	Notes	Single clones*‡	Cells in 2-cell clones*‡§	Total cells*
1a	A4 + L8		PN innervates calyx glomerulus A4 and usually L8	5	5	10
13a	L1	alcohol	2 additional 13a PNs innervate a medial calyx glomerulus, possibly M3	4	5	9
22c	L4	aromatic		2	3	5
24a	L2	aromatic		3	2	5
30a	L6	aromatic	PNs from AL glomerulus 30a innervate either L6 or M4 in calyx	2	2	4
30a	M4	aromatic	PNs from AL glomerulus 30a innervate either L6 or M4 in calyx	2	3	5
33a	l3			1	4	5
33b,47a	D1	ester (47a)		2	5	7
35a	V1	alcohol, aldehyde, ketone		1	6	7
42a	V9¶	alcohol, aldehyde, ketone, ester	V9 newly designated	1	6	7
42b	L9¶	ketone, ester	L9 newly designated	3	1	4
45a	A3 + L11¶	ketone, ester	PN innervates calyx glomerulus A3 and usually L11; L11 newly designated	8	3	11
45b	D4	aromatic	Listed as D4 or D5 by Masuda-Nakagawa et al. (2005)	3	9	12
49a	D3			4	7	11
59a	A5¶	aromatic	A5 newly designated	4	4	8
63a	V5			0	2	2
67b	None	alcohol, aldehyde, ketone, aromatic		0	0	0
74a	None	alcohol		0	0	0
82a	A1			3	2	5
83a	M3			2	0	2
85c	L10¶	alcohol, ketone, ester	L10 newly designated	2	2	4
94b	L3	aromatic	One 94b PN has no calyx innervation	3	11	14
Near 59a	M6¶		Unusual PN, cell body far ventroposteriolateral to other PNs. Axon joins iACT more posterior than other PNs; M6 newly designated	3	0	3
suboesophageal ganglion (SOG)	V3		Not an olfactory PN; does not arborize in the AL	0	8	8

*Each row shows the AL and calyx glomeruli that are consistently connected by individual PNs, together with the number of PNs observed to have that pattern of connectivity.
†From ref. 1.
‡Numbers of cells in clones refer to all GH146-positive cells scored, including the suboesophageal ganglion (SOG) neuron.
§Connectivity in 2-cell clones was inferred by comparison with 1-cell clones that labeled the same AL and calyx glomeruli.
¶These calyx glomeruli are newly designated in this work.

1. Kreher SA, Mathew D, Kim J, Carlson JR (2008) Translation of sensory input into behavioral output via an olfactory system. *Neuron* 59:110–124.

Table S3. Analysis of individual PN clones

Cell	No. cells	AL1	AL2	Cx1	Cx2	Notes
011R	1	1a		A4		
017R	1	1a		A4		
128L	1	1a		A4		
131L	1	1a		A4 + L8		
042R I	2	1a	33b-47a	A4	D1	
071R I	2	1a	49a	A4 + L8	D3	
141R	1	1a		A4		
125L I	2	1a	33a	A4 + L8	I3	
130L I	2	1a	45b	A4 + L8	D4	A 3rd weak PN, not analyzed
130R II	2	1a	42a	A4 + L8	V9	
010L	1	13a		medial, possibly M3		AL-Cx match not consistent with other 13a-L1 PNs
022R	1	13a		L1		
063R	1	13a		L1		
072L	1	13a		L1		
009L II	2	13a	33a	L1	I3	
155R	1	13a		L1		
033R I	2	13a	59a	L1	A5	
095R I	2	13a	45b	L1	D4	
100L I	2	13a	94b	L1	L3	
127L I	2	13a	59a	L1	A5	
145R II	2	13a	94b	medial, possibly M3	L3	AL-Cx match not consistent with other 13a-L1 PNs
007L	1	22c		L4		
048R	1	22c		L4		
041R II	2	22c	33b-47a	L4	D1	
079L II	2	22c	82a	L4	A1	
149R II	2	22c	59a	L4	A5	
098R	1	24a		L2		
101L	1	24a		L2		
120L	1	24a		L2		
121R I	2	24a	SOG	L2	V3	
123R II	2	24a	45b	L2	D4	
036R	1	30a		L6		PN also appears to have a small ventromedial terminal in calyx
094Rb	1	30a		L6		
103R	1	30a		M4		
112R	1	30a		M4		
019R II	2	30a	49a	M4	D3	
074R II	2	30a	49a	M4	D3	
093R I	2	30a	94b	L6	L3	
124R I	2	30a	SOG	L6	V3	
150R II	2	30a	94b	M4	L3	
150L	1	33a		I3		
009L I	2	33a	13a	I3	L1	
062R II	2	33a	59a	I3	A5	
122L II	2	33a	42a	I3	V9	
125L II	2	33a	1a	I3	A4 + L8	
004L	1	33b-47a		D1		
072R	1	33b-47a		D1		
041R I	2	33b-47a	22c	D1	L4	
042R II	2	33b-47a	1a	D1	A4	
043R I	2	33b-47a	49a	D1	D3	
062L II	2	33b-47a	45b	D1	D4	
142R I	2	33b-47a	94b	D1	L3	
147R	1	35a		V1		
014R II	2	35a	45b	V1	D4	
020L I	2	35a	45a	V1	A3 + L11	
037L I	2	35a	63a	V1	V5	
068L I	2	35a	42a	V1	V9	
126L I	2	35a	SOG	V1	V3	
098L I	2	35a	SOG	V1	V3	
146R	1	42a		V9		
013L I	2	42a	SOG	V9	V3	

Cell	No. cells	AL1	AL2	Cx1	Cx2	Notes
068L II	2	42a	35a	V9	V1	
075L I	2	42a	94b	V9	L3	
122L I	2	42a	33a	V9	I3	
130R I	2	42a	1a	V9	A4 + L8	
132R I	2	42a	94b	V9	L3	
080R	1	42b		L9		
096L	1	42b		L9		
157L	1	42b		L9		
102R II	2	42b	45a	L9	A3	
042L	1	45a		A3 + L11		
047L	1	45a		A3 + L11		
060R	1	45a		A3 + L11		
061L	1	45a		A3 + L11		PN also innervates D4, unusual
064R	1	45a		A3		
067R	1	45a		A3 + L11		
090L	1	45a		A3 + L11		
140R	1	45a		A3 + L11		
020L II	2	45a	35a	A3 + L11	V1	
079R I	2	45a	94b	A3 + L11	L3	
102R I	2	45a	42b	A3	L9	
008L	1	45b		D4		weak labeling also in Calyx, probably A1
036L	1	45b		D4		
070L	1	45b		D4		
014R I	2	45b	35a	D4	V1	
044L I	2	45b	63a	D4	V5	
052R II	2	45b	49a	D4	D3	
062L I	2	45b	33b-47a	D4	D1	
075R II	2	45b	94b	D4	L3	
095R II	2	45b	13a	D4	L1	
115R II	2	45b	85c	D4	L10	
123R I	2	45b	24a	D4	L2	
130L II	2	45b	1a	D4	A4 + L8	A 3rd weak PN, not analyzed
031R	1	49a		D3		
050L	1	49a		D3		
061R	1	49a		D3		
111L	1	49a		D3		
019R I	2	49a	30a	D3	M4	
043R II	2	49a	33b-47a	D3	D1	
052R I	2	49a	45b	D3	D4	
071RII	2	49a	1a	D3	A4 + L8	
074L I	2	49a	SOG	D3	V3	
074R I	2	49a	30a	D3	M4	
132L I	2	49a	94b	D3	L3	
035L	1	59a		A4 + L8 or A3 + L11		AL-Cx match not consistent with other 59a PNs
060L	1	59a		A5		A5 split in two parts
078L	1	59a		A5		
107L	1	59a		A5		
156L	1	59a		A5		
033R II	2	59a	13a	A5	L1	
062R I	2	59a	33a	A5	I3	
127L II	2	59a	13a	A5	L1	
149R I	2	59a	22c	A5	L4	
037L II	2	63a	35a	V5	V1	
044L II	2	63a	45b	V5	D4	
011L	1	82a		A1		
031L	1	82a		A1		
051L	1	82a		A1		
079L I	2	82a	22c	A1	L4	
146L I	2	82a	SOG	A1	V3	
001R	1	83a		M3		
009R	1	83a		M3		
101R I	2	85c	94b	L10	L3	
115R I	2	85c	45b	L10	D4	
017L	1	85c		L10		

Cell	No. cells	AL1	AL2	Cx1	Cx2	Notes
092R	1	85c		L10		
047R I	2	94b	SOG	None	V3	No Calyx glomerulus corresponding to AL glomerulus 94b
075L II	2	94b	42a	L3	V9	
075R I	2	94b	45b	L3	D4	
079R II	2	94b	45a	L3	A3 + L11	
093R II	2	94b	30a	L3	L6	
100L II	2	94b	13a	L3	L1	
101R II	2	94b	85c	L3	L10	
132L II	2	94b	49a	L3	D3	
132R II	2	94b	42a	L3	V9	
142R II	2	94b	33b-47a	L3	D1	
040R	1	94b		L3		
043L	1	94b		L3		
145R I	2	94b	13a	L3	medial, possibly M3	
150R I	2	94b	30a	L3	M4	
104R	1	94b		L3		
012L	1	Anterodorsalmedial glomerulus, maybe 83a or 85c		Ventrolateral glomerulus, maybe L10		Could be 85c and L10
066Rb	1	near 59a		M6		
044R	1	near 59a		M6		
065R	1	near 59a		M6		
019L	1	None		M3		No AL arborization
013L II	2	SOG	42a	V3	V9	
074L II	2	SOG	49a	V3	D3	
121R II	2	SOG	24a	V3	L2	
124R II	2	SOG	30a	V3	L6	
146L II	2	SOG	82a	V3	A1	
047R II	2	SOG	94b	V3	None	
098L II	2	SOG	35a	V3	V1	
126L II	2	SOG	35a	V3	V1	

A list of all single projection neurons used to map connections between antennal lobe and calyx glomeruli. Each row shows the analysis of a single labeled cell. The Cell column shows the number of the preparation, the side of the brain, left (L) or right (R), and the number of the cell (I or II) in brain hemispheres with >1 labeled cell; brain hemispheres with >1 labeled cell are therefore listed twice. The No. Cells column shows the number of neurons in the brain hemisphere analyzed, including the GH146-expressing neuron that arborizes in the suboesophageal ganglion (SOG) and innervates calyx glomerulus V3. Columns AL1 and Cx1 list the AL and calyx glomeruli connected by that cell. Columns AL2 and Cx2 list the AL and calyx glomeruli connected by the other labeled cell in the same hemisphere, in the case of 2-cell clones. In brain hemispheres with 2 labeled cells, the matching of the AL and Cx glomeruli is inferred from the matches seen using single-PN clones.